

Degradation relationships for the mechanical properties of corroded steel rebars



Stefania Imperatore^{a,*}, Zila Rinaldi^b, Carlo Drago^a

^a Department of Civil Engineering, "Niccolò Cusano" University of Rome, 00166, Italy

^b Department of Civil Engineering and Computer Science Engineering, University of Rome "Tor Vergata", 00133, Italy

HIGHLIGHTS

- Corrosion effects on the mechanical behavior of reinforcing steel rebars.
- Experimental investigation on the constitutive laws of uniformly corroded steel bars.
- Literature review on the mechanical behavior of locally corroded steel bars.
- Degradation laws for the mechanical properties of corroded reinforcement.

ARTICLE INFO

Article history:

Received 24 January 2017

Received in revised form 18 April 2017

Accepted 27 April 2017

Available online 12 May 2017

Keywords:

Corrosion

Reinforcing steel rebars

Mechanical properties

Degradation equations

ABSTRACT

In the present work the mechanical behavior of reinforcing steel rebars deteriorated by corrosion is investigated. The effects of both the degradation morphologies (uniform and localized) are considered. In particular, an experimental survey on artificially deteriorated steel rebars, with different diameters and subjected to different corrosion degrees, was carried out in the Laboratory of the University of Rome Tor Vergata, in order to obtain a uniform corrosion. The specimens were subsequently subjected to monotonic tensile tests in order to investigate the influence of the uniform corrosion on their constitutive relationships. On the basis of the obtained responses, decay equations for the main mechanical properties are developed. Finally, with reference to the pitting corrosion, the data presented in literature are collected and statistically analyzed for defining, in this case also, degradation equations suitable to estimate the variation of the steel mechanical properties.

© 2017 Elsevier Ltd. All rights reserved.

1. Introduction

The principal cause of deterioration in structural concrete is related to the corrosion of the embedded reinforcement. The corrosion process mainly determines a reduction of the steel cross-section – uniform or localized on the entire reinforcement length – and a worsening of the reinforcing steel strength and ductility properties (Cairns et al. [1], Imperatore and Rinaldi [2], Rinaldi et al. [3], Apostolopoulos and Matikas [4]). Consequently, a reduction of the bearing and dissipative capacity of the structural element occurs (Castel et al. [5], Coronelli and Gambarova [6], Rinaldi et al. [3], Imperatore et al. [7,8], Meda et al. [9], Di Carlo et al. [10,11], Rinaldi et al. [12]). Two different corrosion morphologies can take place, uniform or localized ones, often associated to different degradation processes: carbonation decay (related to

the diffusion of the CO₂ ions into the concrete core) and chloride attack (due to the environmental presence of chlorides), respectively. The hydration products of cement, such as the calcium hydroxide provide a high alkaline environment in concrete that activate a passivating film of iron oxide on the embedded steel bars. This environment protects the steel reinforcement bars from corrosion. Nevertheless, carbon dioxide and moisture at the surface of the concrete can react with these products to produce calcium carbonate, i.e. carbonation of the concrete. When the zone of carbonation extends to the steel, the protective action of the concrete is sharply reduced, due to the reduced PH value of the calcium carbonate. This phenomenon allows the onset of the corrosion in the reinforcing steel. The process of corrosion is accelerated if chloride ions are present. The chlorides do not react chemically in forming rust, but make easier the formation of anodic and cathodic regions in the metal. Under a chloride attack, the protective layer may be destroyed and the bar can be affected by the corrosion process. In both cases (carbonation and chloride phenomena), the steel mechanical properties will decrease. It is then worth defining steel

* Corresponding author.

E-mail address: stefania.imperatore@unicusano.it (S. Imperatore).

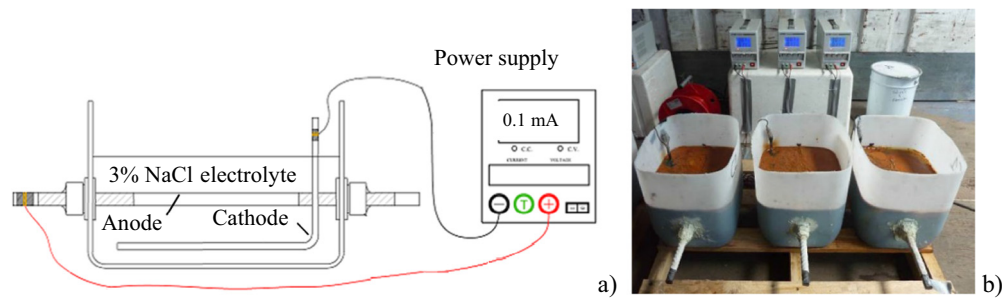


Fig. 1. Accelerated corrosion technique – electrolytic cell: a) scheme; b) experimental set-up.

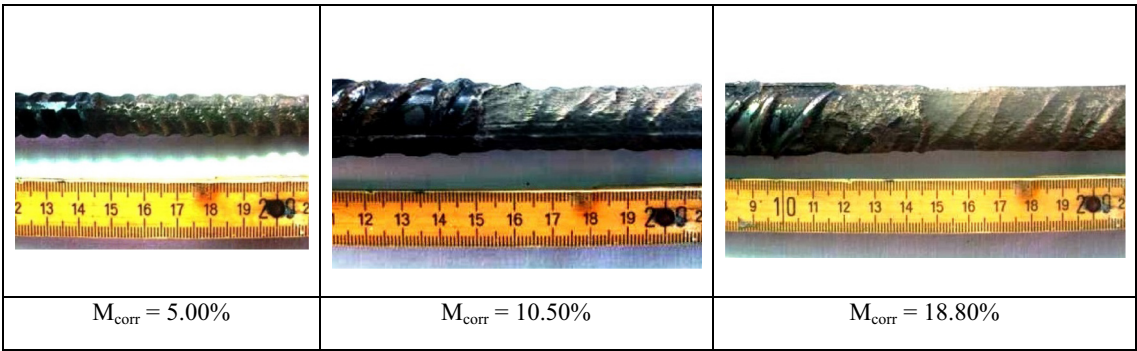


Fig. 2. Uniform corrosion on the artificial damaged specimen.

Table 1
Corrosion degrees of the artificially corroded bare reinforcements.

Ø8	%M _{corr}	Ø12	%M _{corr}	Ø16	%M _{corr}	Ø20	%M _{corr}
A1	0.000	B1	0	C1	0	D1	0
A2	8.97	B2	5.0	C2	4.4	D2	8.8
A3	10.8	B3	8.2	C3	5.3	D3	10.5
A4	19.45	B4	9.4	C4	7.9	D4	10.8
A5	20.63	B5	11.26	C5	8.5	D5	10.8
A6	21.71	B6	14.2	C6	9.0	D6	10.8
A7	22.21	B7	17	C7	10.7	D7	10.83
A8	23.45	B8	17	C8	10.8	D8	11.40
A9	23.65	B9	17.9	C9	10.90	D9	12.7
A10	25.66	B10	18.0	C10	11.00	D10	13.7
A11	25.80	B11	18.5	C11	11.00	D11	14.6
A12	28.55	B12	19.72	C12	11.55	D12	18.3
A13	29.15	B13	24.57	C13	12.20	D13	18.8
A14	53.21	B14	28.68	C14	12.48	D14	19.09
		B15	32.68	C15	12.60	D15	19.4
				C16	19.00	D16	19.79
				C17	19.00	D17	23
				C18	24.00	D18	27.69
				C19	29.00	D19	28.21
				C20	29.00		
				C21	36.00		

degradation equations for the mechanical characteristics of the corroded steel reinforcement, in order to describe the effective sectional capacity of deteriorated elements.

Even if the issue of the degradation in aged reinforced concrete structures attracts a considerable attention, corrosion effects on reinforcing steel mechanical properties are still under study.

The great part of the researches is developed with artificially corroded processes on both bare and embedded rebars. In particular, Almusallam [13] showed, through accelerated experimental tests on steel rebars with strong corrosion localization, that a slight influence on the ultimate strength occurred, but a severe reduction of the ductility took place. The Hellenic researchers assess a signif-

icant improvement to the fieldwork. The degradation of both yield and ultimate tensile strength of the reinforcing bars through artificial corrosion by salt spray was highlighted by (Apostolopoulos et al. [14]) for tempcore Ø8 mm BSt500s, by (Apostolopoulos and Papadopoulos [15]) and (Papadopoulos et al. [16]) for Ø10 mm S400s, Ø12 mm B500c and S500s and by (Alexopoulos et al. [17]) for Ø12 mm BStIV from different manufacturers. Corroded bare bars and embedded reinforcements in aged concrete show significant loss in ductility (Apostolopoulos and Papadakis [18]), magnified when the plastic strains increase (Apostolopoulos and Michalopoulos [19]) and Apostolopoulos and Papadakis [20]. Apostolopoulos et al. [21,22] highlighted that localized (pitting)

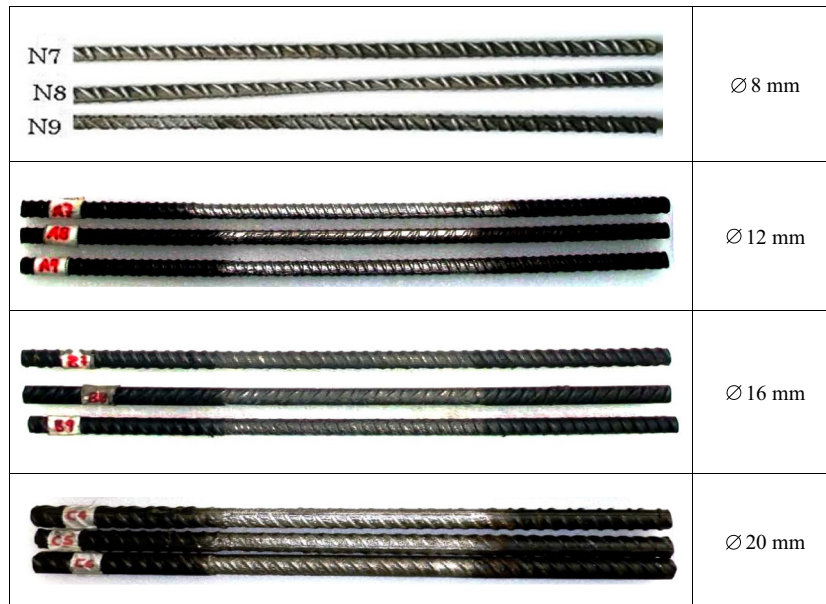


Fig. 3. Some specimen, artificially corroded, before the tensile test.

corrosion causes a degradation larger than the observed for the uniform corrosion. Finally, in the work of Apostolopoulos [23] all the experimental results of the Hellenic researchers are collected. The rate of change of the reinforcement mechanical properties is defined as a function of the corrosion duration and diameter size and a dependence on the reduction of the martensitic layer thickness is detected. The obtained trend is higher than the one recently defined by Ou et al. [24] on artificially corroded reinforcement rebars (probably due to the different characteristics of the Asian steel reinforcement). Moreno et al. [25] tested Ø16 mm and Ø20 mm high ductility reinforcements artificially damaged by different corrosion levels and measured the yield stress, ultimate strength and energy density of deformation decay. The obtained results shows a trend similar to that obtained by the Hellenic researchers. Caprili and Salvatore [26] carried out a wide experimental survey on artificially corroded reinforcement characterized by different steel grades (B400, B450, B500), ductility classes (A, B, C), production processes (TempCore, Micro-Alloyed, Stretched and Cold-Worked) and diameters (Ø8 mm, Ø12 mm, Ø16 mm, Ø20 mm). Both the cyclic and monotonic tests highlight a ductility decrease coupled to a global deterioration of the mechanical properties, when the corrosion level is increased. Fernandez et al. [27] collected a large number of Ø10 mm and Ø12 mm B500SD artificially corroded specimens, performed monotonic and fatigue tests and identified relationships between the corrosion penetration and the steel mechanical properties. Also in this case, the obtained results have the same trend of the Hellenic researchers. Cobo et al. [28] tested B500SD Ø16 mm and Ø20 mm artificially corroded in concrete slab, defining some decay laws by the experimental results.

Fewer researches on naturally corroded steel rebars can be found in literature. According to Maslehuddin et al. [29], sixteen months of atmospheric corrosion did not cause a significant strength reduction on steel reinforcement. On the contrary, Papadopoulos et al. [30] showed the overall decay of the constitutive laws of naturally corroded rebars exposed in coastal areas and subjected to uniform corrosion. Balestra et al. [31] analyzed the mechanical properties of naturally corroded reinforcement buried for 60 years. A comparison between naturally and artificially corroded rebars can be found in Ou et al. [24]. According to this author

the yield and ultimate stresses of the naturally and artificial corroded bars were similar, while the ultimate strain of the naturally corroded bars was smaller than that of the artificially corroded ones. This suggests that the distribution of the cross-sectional areas was more non-uniform in artificially corroded bars than in naturally corroded bars.

The present study intends to investigate both the principal typologies of reinforcing steel degradation in concrete: corrosion by carbonation (uniform) and corrosion by chloride attack (localized). The first morphology is characterized by homogeneous reduction of the steel mechanical properties, the latter by a higher dispersion. In the work, the results of an experimental survey on artificially corroded reinforcement are reported. The artificial corrosion process is carefully calibrated in order to obtain a corrosion shape similar to that observed in naturally corroded structures for carbonation. The results are interpreted also from the microstructural point of view and deterioration equations for the mechanical properties of the corroded reinforcements are defined. The effects of the pitting corrosion is investigated, through an accurate literature review, leading, again to the definition of decay equation for yielding and ultimate stresses and ultimate strain. Finally, the proposed formulations can be usefully adopted in analytical and numerical structural applications.

2. Experimental survey

Aim of this work is the definition of degradation equations for corroded reinforcement steel. As well known, and above reminded, two types of corrosion morphology can develop in R/C structures: uniform corrosion (induced by concrete carbonation) and pitting corrosion (caused by penetration of chlorides and characterized by notches and cavities whose surface and depth increase randomly). Preliminary tests and available studies (Imperatore and Rinaldi [1]; Apostolopoulos and Matikas [4]; Meda et al. [9]) shown that bare bars, after the artificial treatment, exhibit an almost uniform corrosion, comparable to bars naturally corroded by carbonation. On the contrary, steel rebars embedded in a concrete prism, when artificially corroded, present local marked pits. This morphology is typical of natural chloride corrosion.

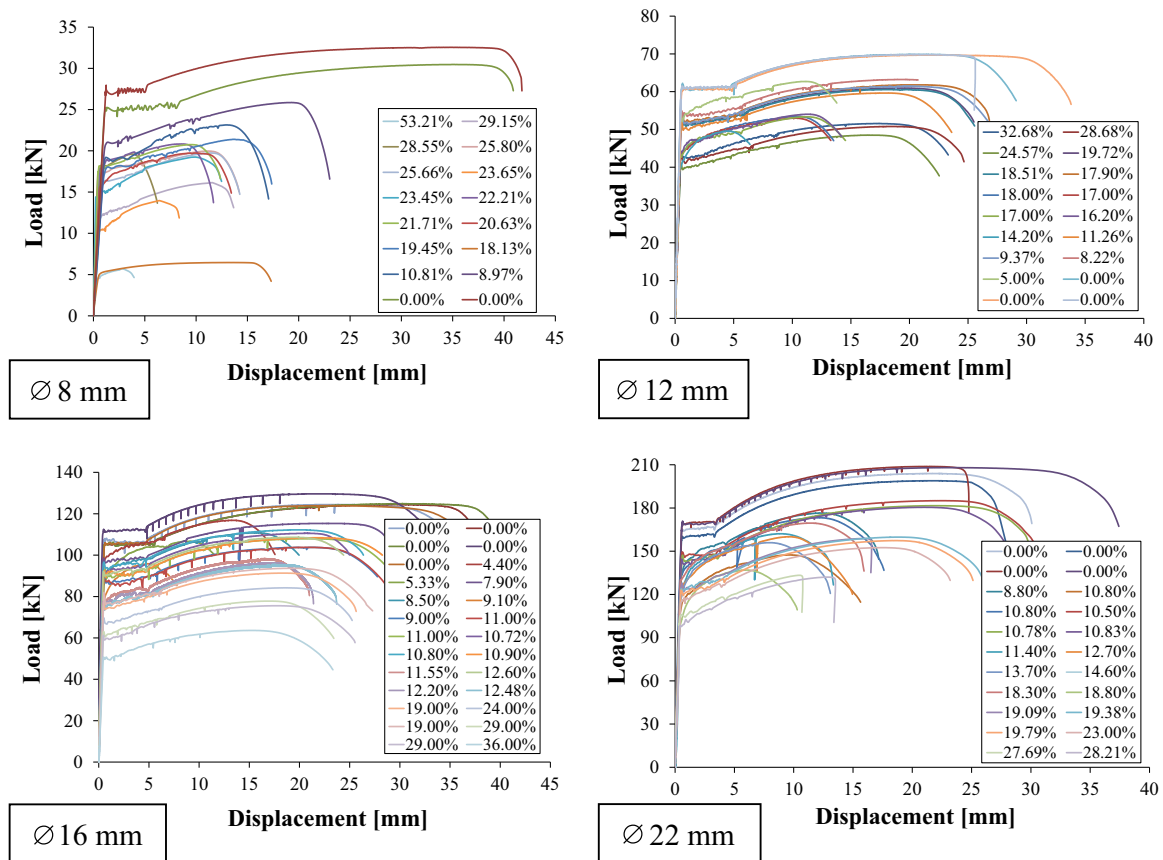


Fig. 4. Load-displacement relationships for the corroded reinforcing steel.

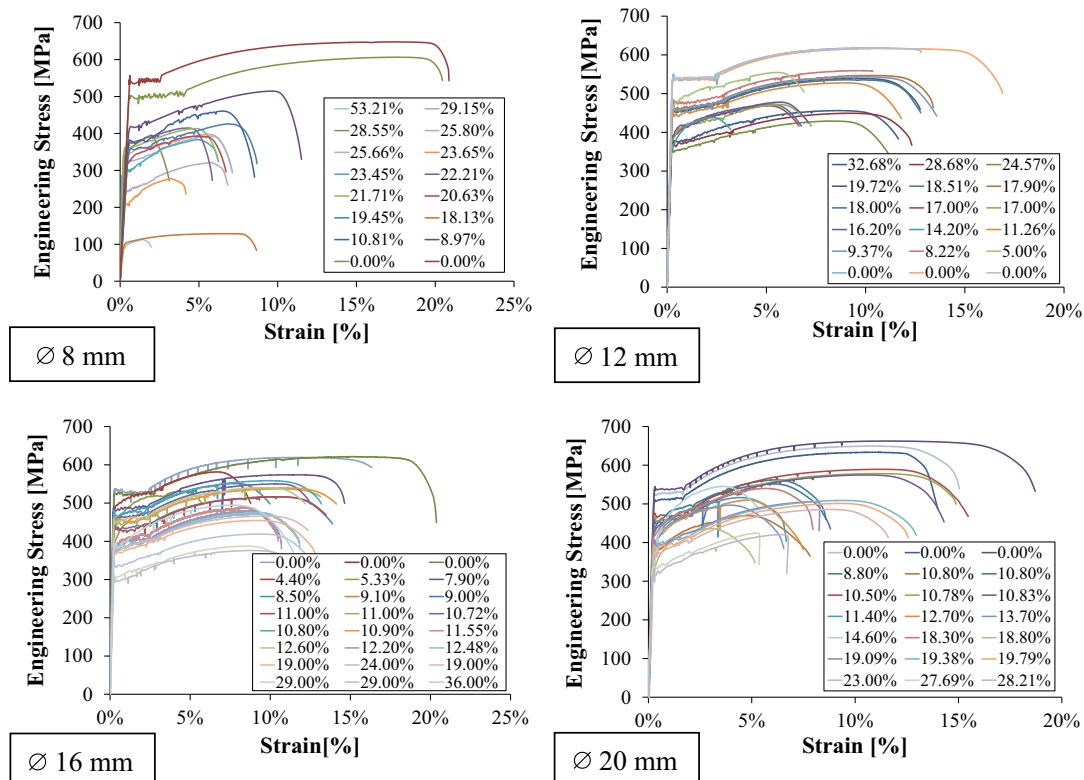


Fig. 5. Stress-strain relationships for the corroded reinforcing steel: engineering stresses.

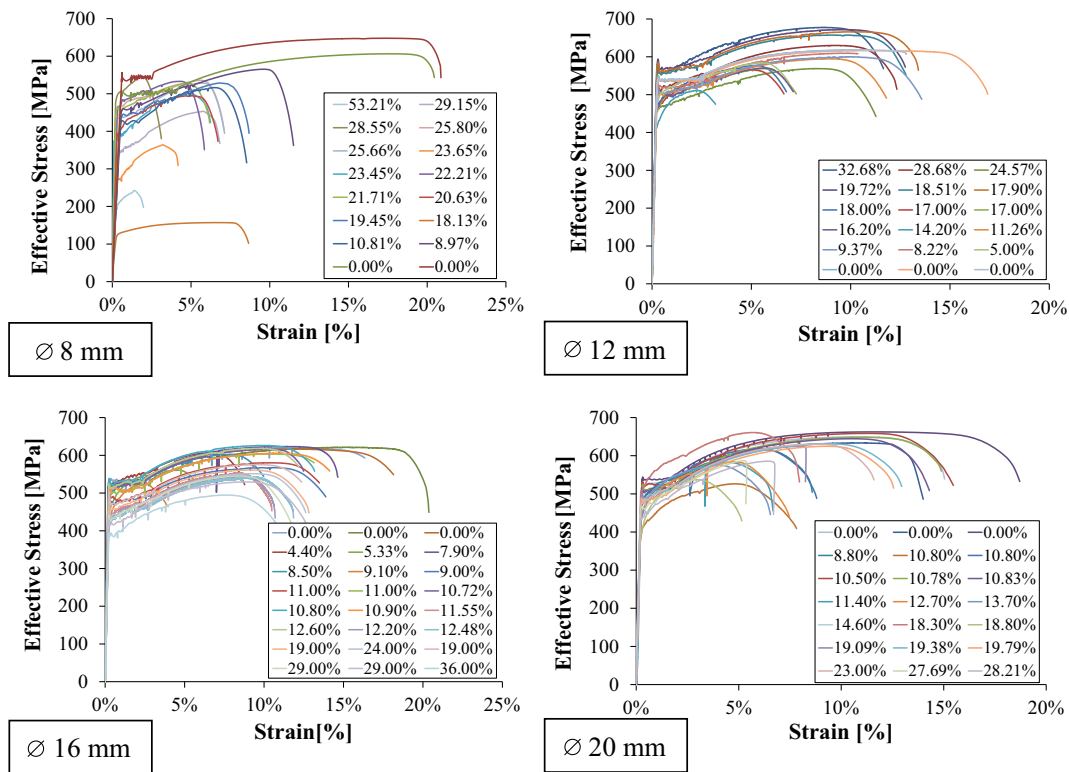


Fig. 6. Stress-strain relationships for the corroded reinforcing steel: effective stresses.

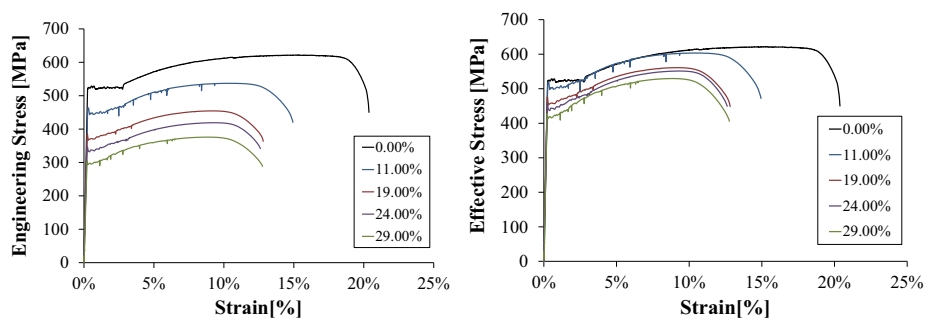


Fig. 7. Stress-strain relationships for Ø16 rebars – detail.

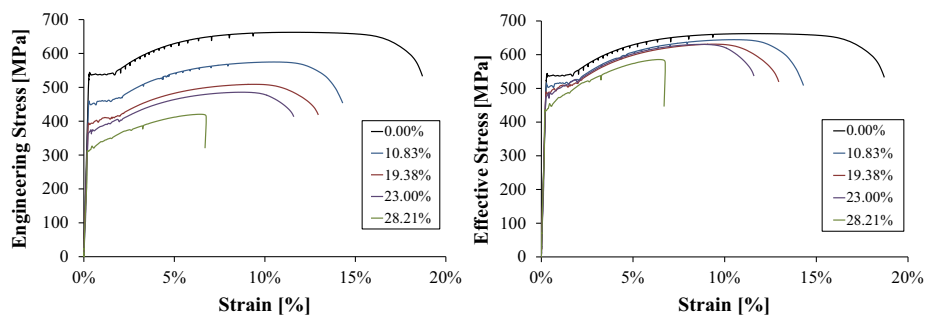


Fig. 8. Stress-strain relationships for Ø20 rebars – detail.

The first part of the present work is mainly focused on the corrosion by carbonation, since it is characterized by a more uniform response. At the aim, experimental tests on artificially deteriorated steel bare reinforcement were carried out in the Laboratory of the University of Rome Tor Vergata.

2.1. Artificial corrosion process

For each specimen, the corrosion was accelerated by impressing a constant anodic current of 0.10 mA, through an integrated system incorporating a DC rectifier with a built-in potentiometer to

Table 2
Mechanical properties of the artificially corroded reinforcing bars.

%Mcorr	Øin	$\sigma_{y \text{ ad}}$ engineering	$\sigma_{u \text{ ad}}$ engineering	$\epsilon_{u \text{ ad}}$ engineering
0.00	8.00	1.00	1.00	1.00
4.40	16.00	0.92	0.94	0.56
5.00	12.00	0.86	0.90	0.51
7.90	16.00	0.91	0.93	0.94
8.22	12.00	0.89	0.91	0.91
8.50	16.00	0.86	0.89	0.65
8.80	20.00	0.82	0.86	0.55
8.97	8.00	0.81	0.82	0.54
9.00	16.00	0.82	0.83	0.87
9.37	12.00	0.85	0.88	0.92
10.50	20.00	0.91	0.90	1.00
10.72	16.00	0.86	0.89	0.86
10.78	20.00	0.90	0.88	0.98
10.80	16.00	0.88	0.90	0.85
10.80	20.00	0.64	0.72	0.43
10.80	20.00	0.81	0.84	0.53
10.81	8.00	0.72	0.73	0.37
10.83	20.00	0.89	0.88	0.93
10.90	16.00	0.84	0.87	0.91
11.00	16.00	0.83	0.83	0.86
11.00	16.00	0.84	0.87	0.86
11.26	12.00	0.83	0.85	0.83
11.40	20.00	0.74	0.79	0.39
11.55	16.00	0.72	0.79	0.68
12.20	16.00	0.71	0.77	0.73
12.48	16.00	0.70	0.77	0.72
12.60	16.00	0.85	0.87	0.82
12.70	20.00	0.74	0.78	0.42
13.70	20.00	0.72	0.76	0.36
14.20	12.00	0.66	0.71	0.20
14.60	20.00	0.65	0.71	0.33
17.00	12.00	0.70	0.76	0.52
17.00	12.00	0.72	0.76	0.48
17.90	12.00	0.86	0.89	0.98
18.00	12.00	0.72	0.77	0.48
18.30	20.00	0.80	0.82	0.51
18.51	12.00	0.84	0.87	0.91
18.80	20.00	0.56	0.67	0.27
19.00	16.00	0.70	0.73	0.77
19.00	16.00	0.72	0.75	0.80
19.09	20.00	0.78	0.77	0.70
19.38	20.00	0.76	0.78	0.84
19.45	8.00	0.69	0.68	0.39
19.72	12.00	0.85	0.87	0.92
19.79	20.00	0.76	0.77	0.82
20.63	8.00	0.61	0.63	0.28
21.71	8.00	0.69	0.66	0.27
22.21	8.00	0.70	0.66	0.25
23.00	20.00	0.70	0.74	0.78
23.45	8.00	0.55	0.61	0.29
23.65	8.00	0.39	0.44	0.18
24.00	16.00	0.63	0.68	0.77
24.57	12.00	0.65	0.70	0.77
25.66	8.00	0.63	0.63	0.32
25.80	8.00	0.67	0.63	0.32
27.69	20.00	0.64	0.65	0.46
28.21	20.00	0.60	0.64	0.56
28.55	8.00	0.69	0.62	0.11
28.68	12.00	0.69	0.73	0.87
29.00	16.00	0.57	0.62	0.71
29.00	16.00	0.56	0.61	0.74
29.15	8.00	0.40	0.51	0.33
32.68	12.00	0.70	0.74	0.80
36.00	16.00	0.48	0.51	0.64
53.21	8.00	0.16	0.18	0.08

control the current intensity. The direction of the current was adjusted so that the reinforcing steel became an anode and a copper plate served as a cathode (Fig. 1). To optimize the process, the specimens were immersed in 3% sodium chloride solution (ASM [32]). Different studies available in literature suggest limiting the current density for accelerated corrosion process of bars embedded

in concrete. In particular Clark & Saifullah [33] and Andrade & Alonso [34] suggested values not higher than 250 and 100- $\mu\text{A}/\text{cm}^2$, respectively. According to these authors, indeed, the limitation is necessary for reproducing the natural environmental conditions and for avoiding negative effects on the steel-concrete bond. In the presented experimental survey, bare bars were subjected to corrosion and no reference is given in literature for this peculiar case. Anyway, the current intensity was chosen in order to be on the line to the suggested ones for embedded bars.

The corrosion by carbonation is simulated on bare bars of different diameters (\varnothing) and length of about 300 mm. The specimens consist in ribbed reinforcing steel bars meeting the requirements of European Standard (S500C in EuroCode2 [35]) artificially corroded up to 50% of mass loss.

The time necessary to obtain the desired damage level is evaluated with a modified Faraday's law (Eq. (1)):

$$\text{time [sec]} = \alpha \cdot \frac{m_{\text{loss}} \cdot n_{\text{specimen}} \cdot C_{\text{Faraday}}}{\text{current[A]} \cdot M_{\text{specimen}}} \quad (1)$$

where m_{loss} is the desired mass loss after the corrosion process, M_{specimen} is the molar mass of the steel reinforcement, n_{specimen} is the steel valence, equal to 2, C_{Faraday} is the Faraday constant, equal to 96480 and α is a constant accounting for the possibility that the corrosive process doesn't start immediately (i.e. equal to 1 for bare bars, and higher than 1 for the embedded specimens).

After the corrosion process, the rebars were cleaned from the rust with 3.5% hydrochloric acid solution (ASTM Standard G1 [36]), and then carefully weighted again. The effective mass loss (M_{loss}) is finally defined, according to Eq. (2), on the basis of the measured weight before and after the corrosion process (m_0 and m_c , respectively):

$$M_{\text{loss}} = \frac{m_0 - m_c}{m_0} \quad (2)$$

Some of the corroded rebars are shown in Fig. 2.

2.2. Mechanical properties of the artificially corroded bare reinforcement

Steel rebars with nominal diameters of $\varnothing 8$ mm, $\varnothing 12$ mm, $\varnothing 16$ mm and $\varnothing 20$ mm, are analyzed, (Table 1 and Fig. 3), for a total number of 80 specimens, characterized by 65 different corrosion degrees, evaluated according to Eq. (2).

After the corrosion process, tensile tests were carried out on the corroded rebars, according to ISO/FDIS 15630-1 [37].

All of the specimens were subjected to monotonic tensile tests, through a Losen Housen Werk servo-hydraulic universal testing machine of 60 ton or an Instron universal testing machine of 10 ton, depending on the rebar diameter. In the tests, always conducted at room temperature with a constant elongation rate of 2 mm/min, each specimen was characterized by gauge length of about 200 mm. The obtained Load-Displacement curves (Fig. 4) were adopted to evaluate the yield and ultimate strength, as well as the elongation to fracture of the corroded reinforcement. The results show that both the yield and the ultimate strengths and the ductility decrease when the corrosion damage is increased for all bars diameters; a more pronounced decay is found for the smallest ones.

The tensile responses are further expressed in terms of stress-strain relationships (Figs. 5 and 6). Specifically, the stress level is calculated considering both the nominal cross sectional area of the steel bars (engineering stresses), and the cross sectional area after the corrosion degradation (effective stresses): in both cases, a decay of the constitutive laws is found. A variation in the reinforcement structure, as will be analyzed into the following, is then

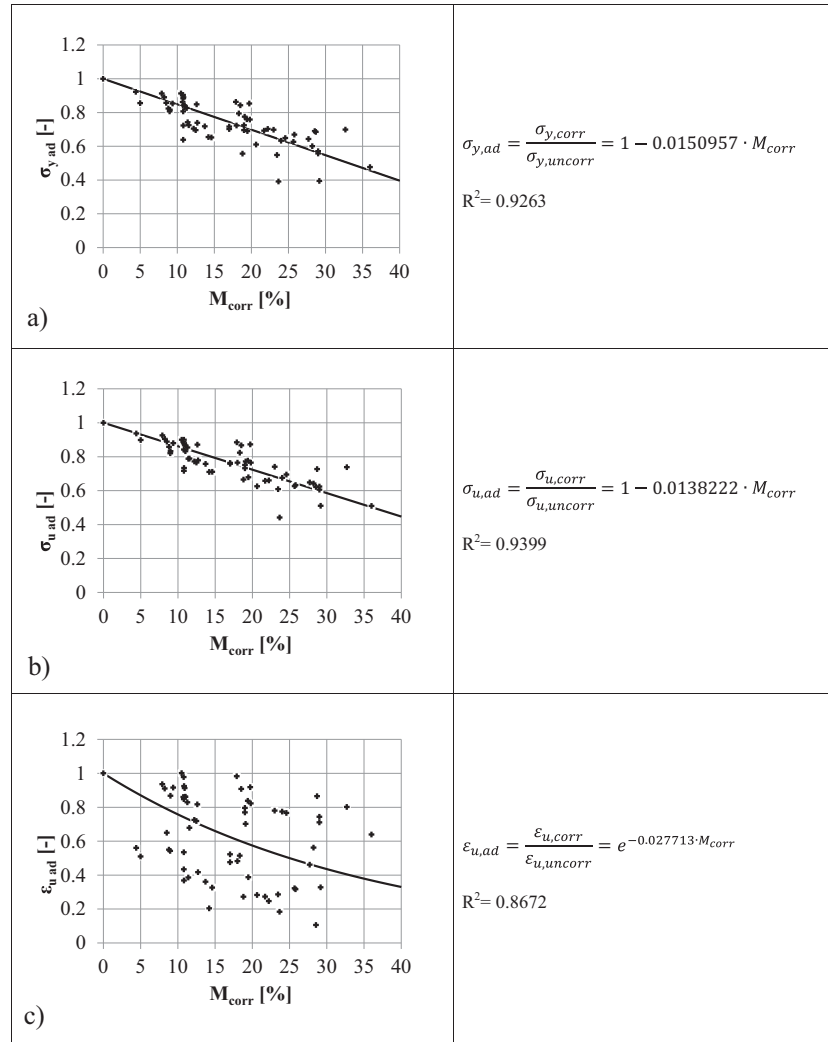


Fig. 9. Mechanical properties degradation of corroded rebars (all the specimens) – dimensionless: a) yielding strength; b) ultimate strength; c) ultimate strain.

deduced. The latter observation is corroborated by the downscaling (up to zero) in the extension of the yield plateau.

According to EuroCode (EN 1990:2002 [38]), in reinforced concrete structures the design value of any geometrical properties is defined as a nominal value. At this aim, the analysis of existing structures or elements should be carried out accounting for the nominal cross-section and not to the after-corrosion cross-section. For this reason, in the following, only the engineering stresses (based on the nominal cross-section) will be considered.

For clarity sake, some of the obtained results for $\varnothing 16$ and $\varnothing 20$ rebars (extracted by Figs 5 and 6) are finally shown in Figs. 7 and 8. The engineering mechanical stresses (evaluated with reference to the nominal cross sectional area of the reinforcement) and the measured ultimate strain are summarized in Table 2 in non-dimensional form with respect to the average un-corroded properties.

3. Statistical interpretation and degradation equations

Based on the obtained results, degradation equations of the steel mechanical properties are defined according to a statistical approach. Specifically, a linear and an exponential regression are identified as best fit for the yielding and ultimate stresses and for the ultimate strain, respectively.

The coefficients of both the linear regression equations are defined by means of the ordinary least squares method (OLS) which allows estimating the coefficient of the linear regression model by assuming a linear form of the data. The sum of the square of the residuals is minimized with the aim to fit an approximated continuous function to a set of data. Then, representing the non-dimensional stresses on the ordinate and the percentage of mass loss on the abscissa axis, the sum of the squares of the residuals is minimized and the decay laws for the yielding and ultimate stresses are defined. A different approach is, instead, considered to evaluate the decay equations for the ultimate strain. In this case, the equation assumes the exponential form:

$$\epsilon_{u,ad} = u + e^{b_1 \cdot M_{corr}} \quad (3)$$

where b_1 is the coefficient to estimate and u are the residuals of the considered curve (null in our case). The method is performed by minimizing the residuals from the considered curve.

The statistical approach is applied both to the single diameters group specimen ($\varnothing 8$ mm, $\varnothing 12$ mm, $\varnothing 16$ mm and $\varnothing 20$ mm, respectively) and to groups of diameters (all the diameters; all the diameters except $\varnothing 8$ mm). In all cases the decay equations are derived and the corresponding R-squared (R^2) coefficient is evaluated. This parameter represents the proportion of the

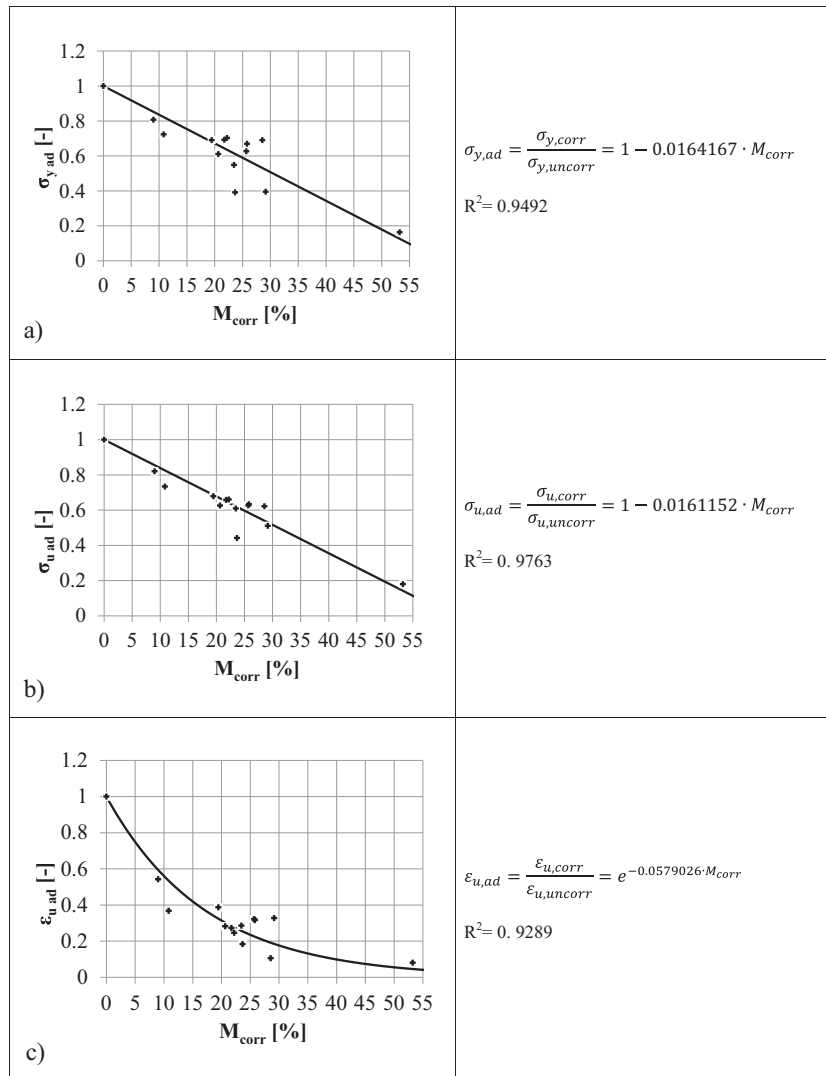


Fig. 10. Mechanical properties degradation of corroded reinforcing steel (Ø8 mm specimens) -: dimensionless; a) yielding strength; b) ultimate strength; c) ultimate strain.

variance in the dependent variable predictable from the independent factor. Then, the coefficient of determination R^2 may be the measurement of the accuracy of the regressions.

The variation of the yielding and ultimate stress, and the ultimate strain, versus the mass loss are reported in Fig. 9 for all the tested specimens. In the Fig. 10 the decay equations are evaluated for the Ø8 mm reinforcement, only. Fig. 11 collects the data for the group of Ø12 mm, Ø16 mm and Ø20 mm rebars, while other estimations are here omitted for sake of brevity.

The obtained trend for the Ø8 mm corroded rebars highlights a significant degradation of the reinforcement mechanical properties, especially pronounced in terms of ductility. This occurrence is explained from the physical point of view. As already highlighted in the technical literature (Apostolopoulos [23], the martensitic layer is smaller in the lower diameter reinforcement (martensite content is the 25%, 30%, 32.5% and 38% for Ø8 mm, Ø10 mm, Ø12 mm and Ø18 mm rebars respectively). The thick martensitic cortex promotes the formation of cavities that quickly intercepts – under a corrosive attack – the lower and weaker core. In this condition, increasing the degradation, the corrosion assumes characteristics similar – but at the same time more regular, since a uniform corrosion occurs globally – to the pitting attack (small variation in strength, great variation in ductility, high dispersion of the results).

Consequently, the proposed degradation equations (Fig. 11) will be related to the diameters in the range Ø12 mm – Ø20 mm.

4. Discussion – corrosion morphology and microstructure considerations

The presented results highlight a worsening of the mechanical properties in the corroded reinforcement ascribed to variations occurring at the microscopic level. A reinforcing steel bars is, in fact, constituted by different layers (martensite, bainite, pearlite, Fig. 12), each one characterized by a different stress-strain law (Kozlov et al. [39]). Specifically, the martensite cortex is stronger, but less ductile, than the inner bainite layer (that may be also weaker than the pearlitic core). The overall reinforcement constitutive law (therefore the reinforcement mechanical properties) strictly depends on the volumetric proportion between these layers. At the same corrosion level (in terms of loss area) the ratio may change significantly in the case of localized corrosion, or may present only little variations in the case of uniform corrosion. This different behavior is schematized in Fig. 13, where the differences in the morphologies of the attack are schematized and emphasized. Obviously, in the real cases, the two morphologies may overlap and

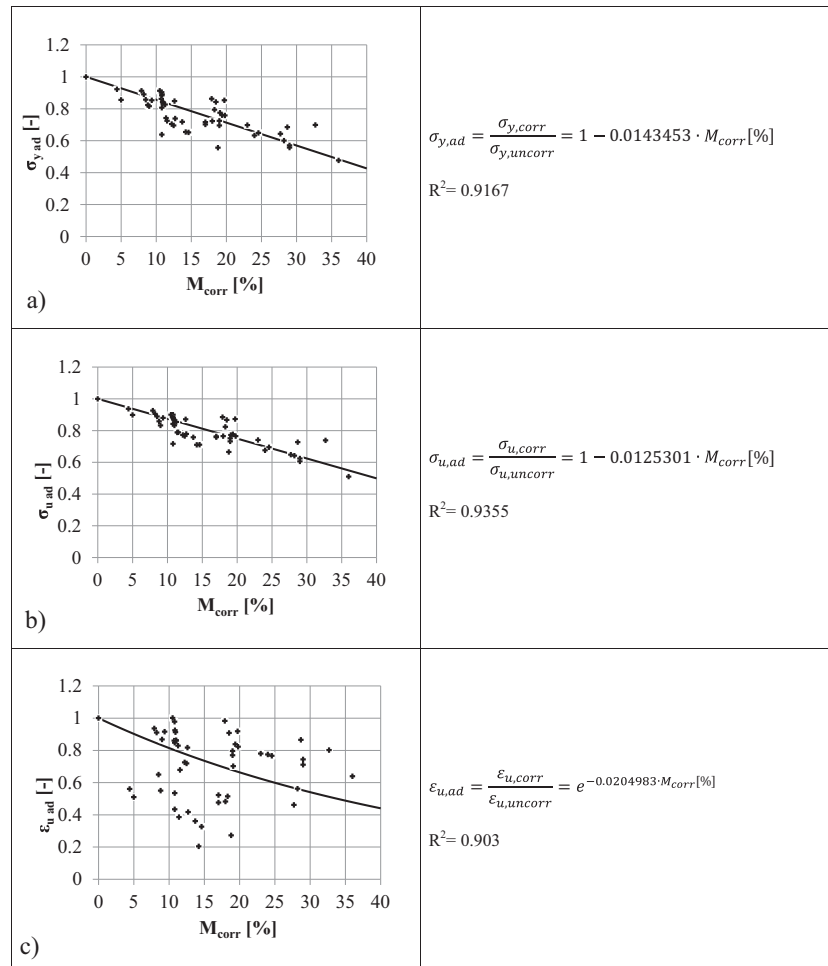


Fig. 11. Mechanical properties degradation of corroded reinforcing steel ($\varnothing 12$ mm, $\varnothing 16$ mm and $\varnothing 20$ mm specimens): dimensionless – a) yielding strength; b) ultimate strength; c) ultimate strain.

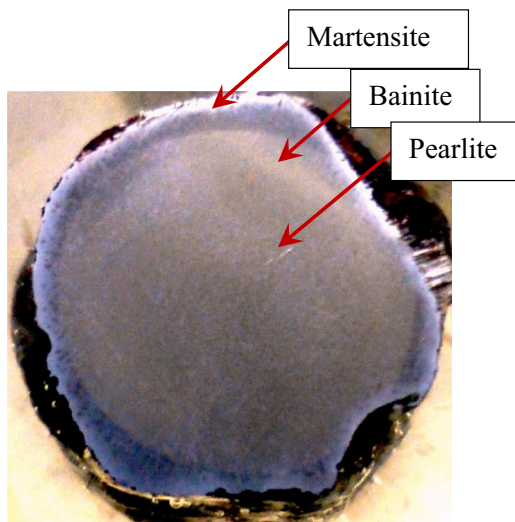


Fig. 12. Metallographic image of a reinforcing bar with the indication of the layers.

when the pitting corrosion occurs, locally also a uniform reduction of the section may be detected.

In the analyzed experimental campaign, characterized by a smooth deterioration, the mass loss is strictly related to the gradual reduction of the martensitic layer (Fig. 14) – which guarantees

hardness and strength – and then to the decrease of the reinforcement mechanical properties. As discussed in the previous section, the overall homogeneity of the experimental results allows defining accurate degradation equations. Instead, in chloride attack the randomly formation of notches causes a variation of the reinforcement mechanical properties related not only to the mass loss, but also to the pits depth and extension (Apostolopoulos and Matikas [4]). This phenomenon leads to a higher scatter in the tensile response.

A great number of experimental data of steel rebars subjected to pitting corrosion, available in literature, have been collected, and statistically analyzed. As a result, degradation equations are developed, according to the procedure highlighted for the uniform corrosion. In Fig. 15 the degradation equations for uniform and pitting corrosion are compared. In the same Figure, the experimental dots, and the related references are reported. The pitting corrosion causes higher reduction of the mechanical properties, with respect to uniform one, in particular in terms of ultimate strain. Furthermore, it has to remark the higher scatter of the experimental results in case of pitting corrosion, (and again mainly in the ultimate strain), due to the influence of the depth and extension of the areas in which the corrosion is localized. These two factors are strictly related to the variation of the volumetric ratio between all the microstructural layers and the localized reduction of the reinforcement cross section, respectively. The first aspect promotes a variation in the combination of the constitutive laws of the layers: due to the specific feature of the single laws, the variation

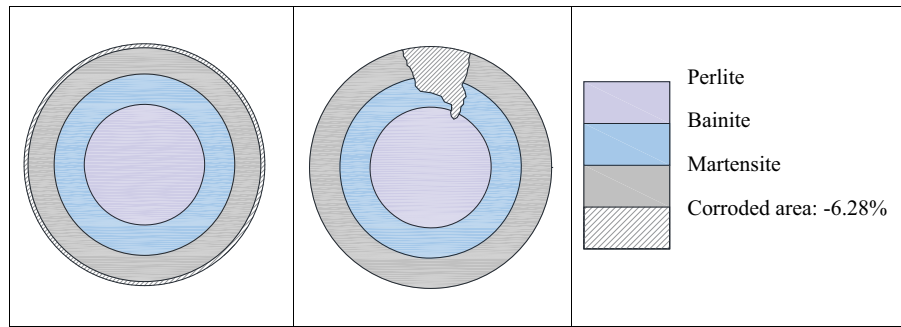


Fig. 13. Difference between uniform (on the left) and localized corrosion (on the right) at the microscopic level: schematization.

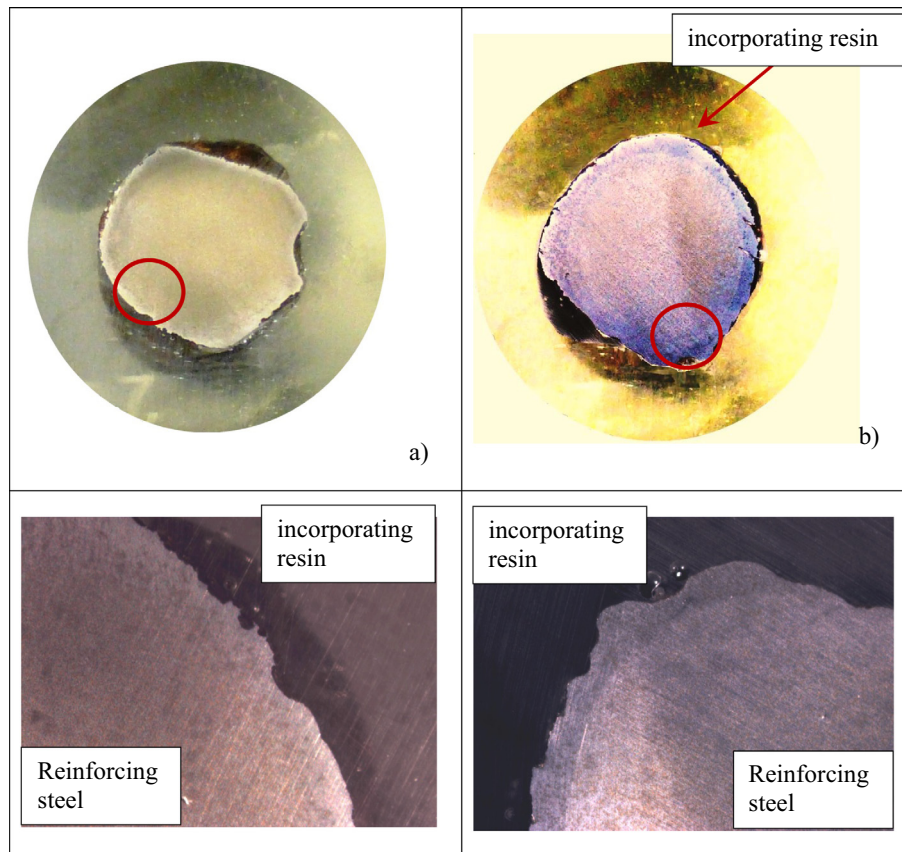


Fig. 14. Difference between uniform (on the left) and localized corrosion (on the right) at the microscopic level: metallographic images on $\varnothing 12$ reinforcing steel rebar artificially corroded. The samples are englobed in resin and chemically etched to reveal the microstructure of the reinforcement.

influences the strength and the ductility, the latter in a significant manner. The reduction of the reinforcement cross section causes the strong localization of the tensional state that can imply the early collapse.

5. Conclusion

In this paper, the results of experimental tensile tests on artificially corroded reinforcement are presented. The goal of the research is the definition of appropriate decay equations for the mechanical properties, useful for modelling the local and global behavior of corroded r.c. elements, through numerical and analytical tools.

Steel rebars with nominal diameters of $\varnothing 8$ mm, $\varnothing 12$ mm, $\varnothing 16$ mm and $\varnothing 20$ mm, for a total number of 80 specimens, characterized by 65 different corrosion degrees, were analyzed. In order to obtain an overall homogeneity of the experimental results, uniform corrosion was simulated with an accelerated corrosion process on bare bars.

Finally, tensile tests were carried out and the obtained responses were compared and discussed. For all the considered specimen, a reduction of the mechanical properties, increasing the corrosion level is shown, and a sharp decrease of the yield plateau is observed. A significant degradation in terms of ductility is detected mainly for smaller reinforcement diameter (i.e. 8 mm). The reason is ascribed to a significant change of the volumetric ratio between the microscopic layers (martensite, bainite, pearlite).

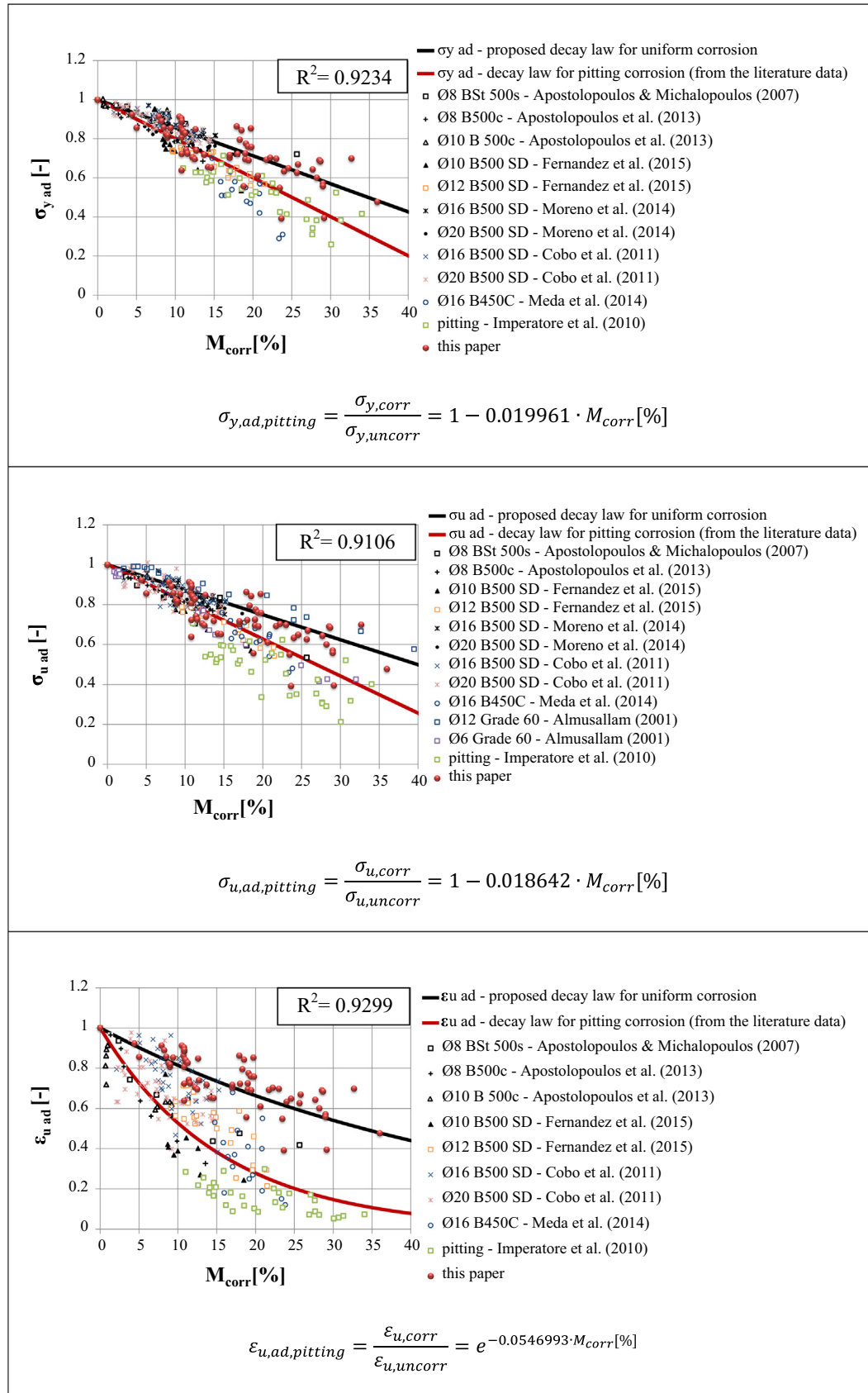


Fig. 15. Degradation equations of reinforcing steel affected by pitting corrosion (from the data of a literature review) and comparison with the degradation equations defined for uniformly corroded reinforcing steel.

To define appropriate degradation equations, the strength and strain experimental data are converted in non-dimensional form and synthesized in linear and exponential regressions (for the yielding and ultimate stresses and for the ultimate strain, respectively) according to a statistical approach, as a function of the corrosion level, expressed in terms of mass loss. In the study, only the engineering mechanical properties (calculated with reference to the nominal cross sectional area of the reinforcement) are considered, as motivated in the paper. The knowledge of the engineering properties, can be useful in analytical or numerical model, in order to modify the constitutive laws of the corroded reinforcement, without reducing the steel diameter. Decay equations for the uniform corrosion are then defined, based on the statistical approach, applied to the experimental results presented in the study.

Finally, the same statistical approach is developed for the analysis of the mechanical properties of the steel rebars, affected by pitting corrosion, based on the experimental data available in literature.

The relationships can be summarized as follows:

Degradation equations for uniform corrosion (from experimental results)

$$\begin{aligned}\frac{\sigma_{y,corr}}{\sigma_{y,uncorr}} &= 1 - 0.0143453 \cdot M_{corr}[\%] \\ \frac{\sigma_{u,corr}}{\sigma_{u,uncorr}} &= 1 - 0.0125301 \cdot M_{corr}[\%] \\ \frac{E_{u,corr}}{E_{u,uncorr}} &= e^{-0.0204983 \cdot M_{corr}[\%]}\end{aligned}\quad (4)$$

Degradation equations for pitting corrosion (from a literature review)

$$\begin{aligned}\frac{\sigma_{y,corr}}{\sigma_{y,uncorr}} &= 1 - 0.019961 \cdot M_{corr}[\%] \\ \frac{\sigma_{u,corr}}{\sigma_{u,uncorr}} &= 1 - 0.018642 \cdot M_{corr}[\%] \\ \frac{E_{u,corr}}{E_{u,uncorr}} &= e^{-0.0546993 \cdot M_{corr}[\%]}\end{aligned}\quad (5)$$

Acknowledgment

The authors thank prof. Ilaria Cacciotti who carried out the metallographic investigation.

References

- [1] J. Cairns, G.A. Plizzari, Y. Du, D.W. Law, C. Franzoni, Mechanical properties of corrosion-damaged reinforcement, *ACI Mater. J.* 102 (4) (2005) 256–264. art. no. 102–M29.
- [2] S. Imperatore, Z. Rinaldi, Mechanical behaviour of corroded rebars and influence on the structural response of R/C elements. Concrete Repair, Rehabilitation and Retrofitting II: 2nd International Conference on Concrete Repair, Rehabilitation and Retrofitting, ICCRRR-2, 24–26 November 2008, Cape Town, South Africa (p. 203). CRC Press, 2008.
- [3] Z. Rinaldi, S. Imperatore, C. Valente, Experimental evaluation of the flexural behavior of corroded P/C beams, *Constr. Build. Mater.* 24 (11) (2010) 2267–2278.
- [4] A. Apostolopoulos, T.E. Matikas, Corrosion of bare and embedded in concrete steel bar—impact on mechanical behavior, *Int. J. Struct. Integrity* 7 (2) (2016) 240–259.
- [5] A. Castel, R. Francois, G. Arligue, Mechanical behaviour of corroded reinforced concrete beams – Part 1: experimental study of corroded beams. *Mater Struct/Mater et Constr* 2000:33. November.
- [6] D. Coronelli, P.G. Gambarova, Structural assessment of corroded reinforced concrete beams: modeling guidelines, *ASCE – J. Struct. Eng.* 130 (8) (2004) 1214–1224.
- [7] S. Imperatore, A. Leonardi, Z. Rinaldi, Mechanical behaviour of corroded rebars in reinforced concrete elements. *Mechanics, Models and Methods in Civil Engineering*, 2012, 207–220.
- [8] S. Imperatore, A. Leonardi, Z. Rinaldi, Strength decay of RC sections for chloride attack, *Int. J. Struct. Integrity* 7 (2) (2016) 194–212.
- [9] A. Meda, S. Mostosi, Z. Rinaldi, P. Riva, Experimental evaluation of the corrosion influence on the cyclic behaviour of RC columns, *Eng. Struct.* 76 (2014) 112–123.
- [10] F. Di Carlo, A. Meda, Z. Rinaldi, Numerical Modelling of Corroded RC Columns Repaired with High Performance Fiber Reinforced Concrete Jacket. *Key Engineering Materials*. Vol. 711. Trans Tech Publications, 2016, 2016.
- [11] F. Di Carlo, A. Meda, Z. Rinaldi, Cyclic behavior of RC columns repaired with HPFRC jackets, in: *Proceedings of Italian Concrete Days, Giornate AICAP 2016* Congresso CTE, Evoluzione e Sostenibilità delle Strutture in Calcestruzzo, Roma, 27–28 Ottobre 2016, 2016.
- [12] Z. Rinaldi, C. Valente, L. Pardi, A simplified methodology for the evaluation of the residual life of corroded elements. 2008 *Structure and Infrastructure Engineering*, 4 (2), pp. 139–152 Taylor & Francis Eds.
- [13] A.A. Almusallam, Effect of degree of corrosion on the properties of reinforcing steel bars, *Constr. Build. Mater.* 15 (2001) 361–368.
- [14] Ch. Alk. Apostolopoulos, M.P. Papadopoulos, Sp.G. Pantelakis, Tensile behavior of corroded reinforcing steel bars BSt 500s, *Constr. Build. Mater.* 20 (2006) 782–789.
- [15] C. Alk. Apostolopoulos, M.P. Papadopoulos, Tensile and low cycle fatigue behavior of corroded reinforcing steel bars S400, *Constr. Build. Mater.* 21 (2007) 855–864.
- [16] M.P. Papadopoulos, C. Alk. Apostolopoulos, N.D. Alexopoulos, Sp.G. Pantelakis, Effect of salt spray corrosion exposure on the mechanical performance of different technical class reinforcing steel bars, *Mater. Des.* 28 (2007) 2318–2328.
- [17] N.D. Alexopoulos, C. Alk. Apostolopoulos, M.P. Papadopoulos, Sp.G. Pantelakis, Mechanical performance of BStIV grade steel bars with regard to the long-term material degradation due to corrosion damage, *Constr. Build. Mater.* 21 (6) (2007) 1362–1369.
- [18] C. Alk. Apostolopoulos, V.G. Papadakis, Consequences of steel corrosion on the ductility properties of reinforcement bar, *Constr. Build. Mater.* 22 (12) (2008) 2316–2324.
- [19] C. Apostolopoulos, D. Michalopoulos, The impact of corrosion on the mechanical behavior of steel undergoing plastic deformation, *Mater. Corros.* 58 (1) (2007) 5–12.
- [20] C. Alk. Apostolopoulos, V.G. Papadakis, Mechanical behavior of reinforcement stirrups BSt 500s at corrosive environment, *J. Mater. Eng. Perform.* 16 (2) (2007) 236–241.
- [21] C. Alk. Apostolopoulos, S. Demis, V.G. Papadakis, Chloride-induced corrosion of steel reinforcement—Mechanical performance and pit depth analysis, *Constr. Build. Mater.* 38 (2013) 139–146.
- [22] C. Alk. Apostolopoulos, T.E. Matikas, C. Apostolopoulos, G. Diamantogiannis, Pit corrosion examination of bare and embedded steel bar, in: 10th International Scientific and Technical Conference, Advanced Metal Materials and Technologies (AMMT'2013), Saint Petresburg, June 25–29, pp. 489–495, 2013.
- [23] C. Alk. Apostolopoulos, The influence of corrosion and cross-section diameter on the mechanical properties of B500c steel, *J. Mater. Eng. Perform.* 18 (2) (2009) 190–195.
- [24] Y.C. Ou, Y.T.T. Susanto, H. Roh, Tensile behavior of naturally and artificially corroded steel bars, *Constr. Build. Mater.* 103 (2016) 93–104.
- [25] E. Moreno, A. Cobo, G. Palomo, M.N. González, Mathematical models to predict the mechanical behavior of reinforcements depending on their degree of corrosion and the diameter of the rebars, *Constr. Build. Mater.* 61 (2014) 156–163.
- [26] S. Caprili, W. Salvatore, Cyclic behaviour of uncorroded and corroded steel reinforcing bars, *Constr. Build. Mater.* 76 (2015) 168–186.
- [27] I. Fernandez, J.M. Bairán, A.R. Marí, Corrosion effects on the mechanical properties of reinforcing steel bars. Fatigue and σ – ϵ behavior, *Constr. Build. Mater.* 101 (2015) 772–783.
- [28] A. Cobo, E. Moreno, M.F. Canovas, Mechanical properties variation of B500SD high ductility reinforcement regarding its corrosion degree, *Mater. Constr.* 61 (304) (2011) 517–532.
- [29] M. Maslehuddin, I.M. Allam, G.J. Al-Sulaimani, A.I. Al-Mana, S.N. Abdujauwad, Effect of rusting of reinforcing steel on its mechanical properties and bond with concrete, *ACI Mater. J.* 87 (5) (1990) 496–502.
- [30] M.P. Papadopoulos, C. Alk. Apostolopoulos, A.D. Zervaki, G.N. Haidemenopoulos, Corrosion of exposed rebars, associated mechanical degradation and correlation with accelerated corrosion tests, *Constr. Build. Mater.* 25 (8) (2011) 3367–3374.
- [31] C. Balestra, M. Lima, A. Silva, R. Medeiros-Junior, Corrosion degree effect on nominal and effective strengths of naturally corroded reinforcement, *J. Mater. Civ. Eng.* (2016), [http://dx.doi.org/10.1061/\(ASCE\)MT.1943-5533.0001599](http://dx.doi.org/10.1061/(ASCE)MT.1943-5533.0001599), 04016103.
- [32] ASM International, ASM Handbook Volume 13A: Corrosion: Fundamentals, Testing, and Protection. Editor: Stephen D. Cramer and Bernard S. Covino, Jr. ISBN: 978-0-87170-705-5, 2013.
- [33] M. Saifullah, L.A. Clark, Effect of corrosion rate on the bond strength of corroded reinforcement, in: *Proceedings of International Conference on Corrosion and Corrosion Protection of Steel in Concrete* vol. 1, pp. 591–602, 1994, July.
- [34] C. Andrade, C. Alonso, Corrosion rate monitoring in the laboratory and on-site, *Constr. Build. Mater.* 10 (5) (1996) 315–328.
- [35] EN 1992-1 1. EuroCode 2: Design of concrete structures –Part 1-1: General rules and rules for buildings, 2004.
- [36] ASTM Standard G1-90, Standard Practice for Preparing, Cleaning, and Evaluating Corrosion Test Specimens, ASTM International, West Conshohocken, PA, 2011.
- [37] ISO/FDIS 15630-1, International standard. Steel for the reinforcement and prestressing of concrete – test methods. Part 1: reinforcing bars, wire rod and wire, 2002.
- [38] EN 1990:2002(E). EuroCode: Basis of Structural Design, 2002.
- [39] É.V. Kozlov, A.V. Plevkov, A.B. Yur'ev, V.E. Gromov, Stress-strain curves, fracture mechanisms, and size effect for low-carbon low-alloyed steels with a quasi-composite structure, *Russ. Phys. J.* 45 (3) (2002) 261–273.